Estimating CRTM-simulated Measurement Uncertainties and their Impact on Detecting and Analyzing NOAA Operational MW Sounder Calibration Anomalies

National Environmental Satellite, Data, and Information Service

GSICS MW Subgroup Meeting
25 January 2023

Siena Iacovazzi[1],*, Quanhua Liu[2] , Hu Yang[3], James Fuentes[4], and Ninghai Sun[1]

[1]GST, Inc., 7501 Greenway Center Drive, Suite 1100, Greenbelt, MD 20770 USA; *Siena.Iacovazzi@noaa.gov; Ninghai.Sun@noaa.gov

[2]NOAA/NESDIS/STAR, 5830 University Research Court, College Park, MD 20740 USA; Quanhua.Liu@noaa.gov

[3]Cooperative Institute of Earth System Studies, University of Maryland, College Park, MD, 20740 USA; Hu.Yang@noaa.gov

[4]Northrop Grumman, Azusa Facility, 1111 W 3rd St, Azusa, CA 91702 USA; james.fuentes@ngc.com

Outline

- Using Community Radiative Transfer Model (CRTM) simulated microwave (MW) brightness temperatures (Tb) to monitor and evaluate space-based MW sensor data performance
- Dominant MW instrument calibration anomaly mechanisms
- Method to estimate CRTM-simulated Tb uncertainties and their relative size to calibration anomalies

Harnessing CRTM-simulated MW Tb

- ❖ CRTM-simulated background (B) MW sounder Tb values can be subtracted from collocated observed (O) instrument Ta values to form single-sensor O-B Ta bias estimates
- ❖ Double differences of O-B Ta bias between MW instrument pairs can estimate inter-sensor Ta biases
- ❖ These parameters are used to monitor NOAA operational MW sounder data quality and analyze instrument calibration anomalies*

*Iacovazzi, R.; L. Lin; N. Sun; Q Liu, 2020. https://doi.org/10.3390/rs12050828
Iacovazzi *et al.* Terres., Atmos. and Ocn. Sci., 2022. https://doi.org/10.1007/s44195-022-00008-0

Common Sources of NOAA Operational MW Sounder Calibration Anomalies

Cold
Space

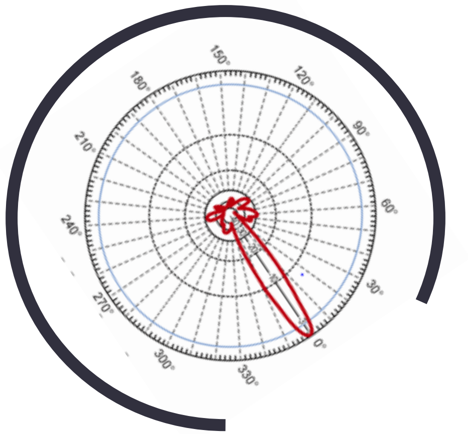

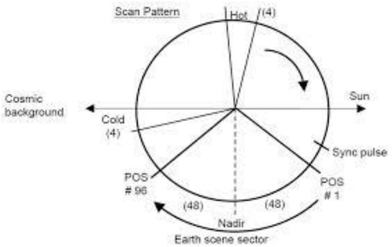

2.67 second rotation

- ❖ **NOAA Operational MW Sounder 3-point Calibration System Includes measurements of**
  - Warm load with NIST-Traceable Platinum Resistance Thermometers (~275 K – 285 K)
  - Cold Space (~2.73 K)
  - Earth Scene
- ❖ **MW Antenna Reflectors Characteristics Related to Calibration Anomalies**
  - Response in the sidelobes (SLs) beyond the main lobe
  - Non-zero emissivity at the reflector temperature

Common Sources of NOAA Operational MW Sounder Calibration Anomalies

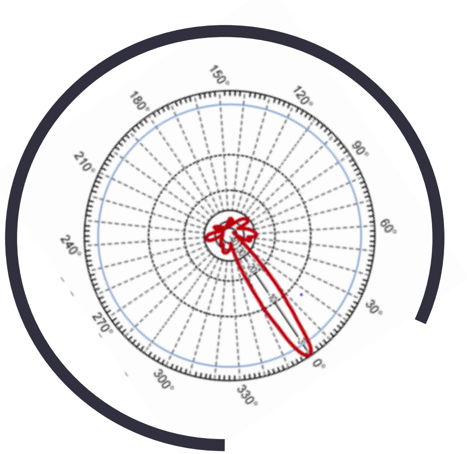

Cold
Space

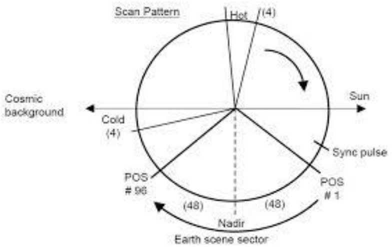

2.67 second rotation

- **NOAA Operational MW Sounder 3-point Calibration System Includes measurements of**
  - Warm load with NIST-Traceable Platinum Resistance Thermometers (~275 K – 285 K)
  - Cold Space (~2.73 K)
  - Earth Scene
- **MW Antenna Reflectors Characteristics Related to Calibration Anomalies**
  - Response in the sidelobes (SLs) beyond the main lobe
  - Non-zero emissivity at the reflector temperature
- **Earth View:**
  - Antenna emission and earth radiance absorption
  - Earth radiance in antenna SL

Common Sources of NOAA Operational MW Sounder Calibration Anomalies

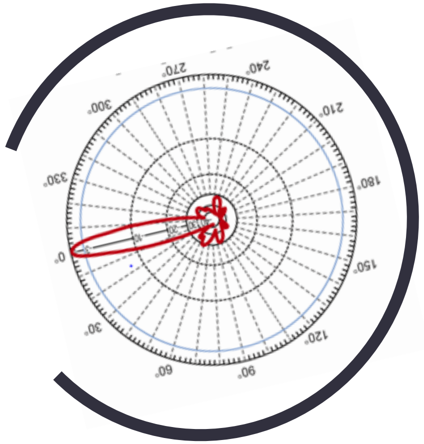

Cold
Space

- **Cold Space View:**
  - Antenna emission
  - Earth and satellite radiance in antenna SL

- **NOAA Operational MW Sounder 3-point Calibration System Includes measurements of**
  - Warm load with NIST-Traceable Platinum Resistance Thermometers (~275 K – 285 K)
  - Cold Space (~2.73 K)
  - Earth Scene
- **MW Antenna Reflectors Characteristics Related to Calibration Anomalies**
  - Response in the sidelobes (SLs) beyond the main lobe
  - Non-zero emissivity at the reflector temperature

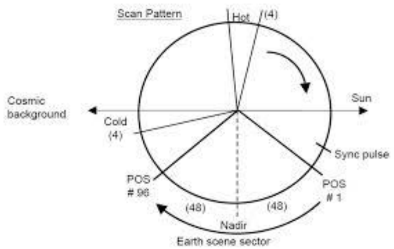

2.67 second rotation

- **Earth View:**
  - Antenna emission and earth radiance absorption
  - Earth radiance in antenna SL

Common Sources of NOAA Operational MW Sounder Calibration Anomalies

- **NOAA Operational MW Sounder 3-point Calibration System Includes measurements of**
  - Warm load with NIST-Traceable Platinum Resistance Thermometers (~275 K – 285 K)
  - Cold Space (~2.73 K)
  - Earth Scene
- **MW Antenna Reflectors Characteristics Related to Calibration Anomalies**
  - Response in the sidelobes (SLs) beyond the main lobe
  - Non-zero emissivity at the reflector temperature

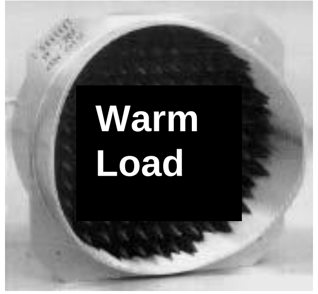

- **Warm Load View:**
  - Antenna emission and Warm Load radiance absorption

Cold Space

- **Cold Space View:**
  - Antenna emission
  - Earth and satellite radiance in antenna SL

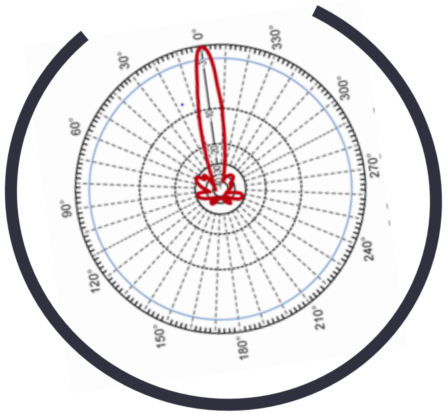

- **Earth View:**
  - Antenna emission and earth radiance absorption
  - Earth radiance in antenna SL

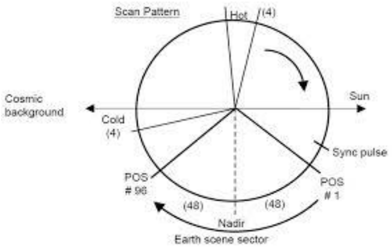

2.67 second rotation

Calibration Radiance Contribution Normalized Magnitudes

Radiance Contribution Mechanism	Instr Type	Single Sensor NSF*	Inter-sensor NSF ATMS-to-AMSU-A
Earth radiance in earth scene antenna SL	ATMS	(1) ~10^{-2}	~10^{-4}
	AMSU-A	~10^{-2}	
Earth radiance in cold space view antenna SL	ATMS	~10^{-3}	~10^{-4}
	AMSU-A	~10^{-3}	
Reflected earth radiance from the satellite in cold space view antenna SL	ATMS	~10^{-3}	~10^{-4}
	AMSU-A	~10^{-3}	
Antenna emission in the cold space view	ATMS	~10^{-4}	(2) ~10^{-3}
	AMSU-A	~10^{-3}	
Warm load radiance absorption by the antenna	ATMS	~10^{-4}	~10^{-3}
	AMSU-A	~10^{-3}	
Antenna emission in the warm load view	ATMS	~10^{-4}	~10^{-3}
	AMSU-A	~10^{-3}	
Earth radiance absorption by the antenna	ATMS	~10^{-4}	~10^{-3}
	AMSU-A	~10^{-3}	
Antenna emission in the earth view	ATMS	~10^{-4}	~10^{-3}
	AMSU-A	~10^{-3}	
CRTM Tb Uncertainty	ATMS	(3) ??	?? ??
	AMSU-A	??	X ??

***Normalized Scaling Factor (NSF) is the magnitude of a radiance contribution relative to the radiance of a 300 K object.**

1. Inter-sensor NSF can be smaller than the single-sensor NSF by one or more orders of magnitude.
2. Larger ATMS-to-AMSU-A NSF residuals are due to neglected non-zero antenna emissivity impacts.
3. Simulated Tb uncertainties have not been quantified.

Estimating CRTM-simulated Tb Uncertainty (1 of 2)

1. Consider regions of interest (ROIs) from 60°S to 60°N that utilize the simplest CRTM physics
   a) Rain-free
   b) Ocean-only for MW window channels and surface-influenced sounding channels, and global for sounding channels free of surface influence
   c) Near-nadir only
2. CRTM-simulated Tb uncertainties are assumed to have a relatively strong linear relationship with at-sensor radiance, except at the coldest temperatures
3. This study focuses on
   a) Single-sensor NOAA operational ATMS Chs 2-3 and 5-15/AMSU-A Chs 4-14 (monitored at NOAA/NESDIS/STAR using BOTH Global Navigation Satellite System (GNSS) Radio Occultation (RO) and ECMWF Ensemble (ENS) NWP soundings)
   b) Inter-sensor ATMS-to-AMSU-A statistics formed from single-sensor instrument pairs.

Estimating CRTM-simulated Tb Uncertainty (2 of 2)

1 Day of GNSS RO Sounding Time and Lat/Lon
- COSMIC-1, KOMPSAT-5, and COSMIC-2

ECMWF 51-member ENS NWP Gridded, 6-hourly Sounding Time and Lat/Lon

Collocate Data

MW Sounder Observed Ta Data Time and Lat/Lon
- ATMS Chs 2-3, 5-15: S-NPP and NOAA-20
- AMSU-A Chs 2-14: NOAA-18 and -19, Metop-A to -C

ECMWF T and WV Soundings @ Collocations

Simulate Tb with CRTM

Simulate Tb with CRTM

GNSS-RO T and WV Soundings @ Collocations
- COSMIC-1, KOMPSAT-5, and COSMIC-2

ECMWF ENS and GNSS RO Sounding and CRTM-simulated Tb Data Analysis

ECMWF ENS and GNSS RO Sounding Comparison

Single-sensor $Tb_{ECMWF} - Tb_{RO}$ for each MW sounder

Inter-sensor Tb bias created from MW sounder pair $Tb_{ECMWF} - Tb_{RO}$ double differences

Global-average, ECMWF and RO Sounding Differences

Temp difference profile at matchups between ECMWF, GNSS RO, and MW sounder data.

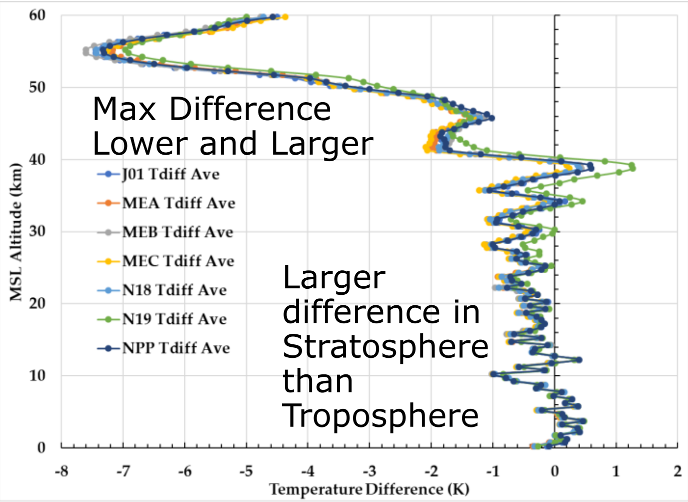

Jan 1, 2020

ATMS Ch 15/ AMSU-A Ch 14

ATMS Ch 10/ AMSU-A Ch 9

ATMS/AMSU-A Ch 2

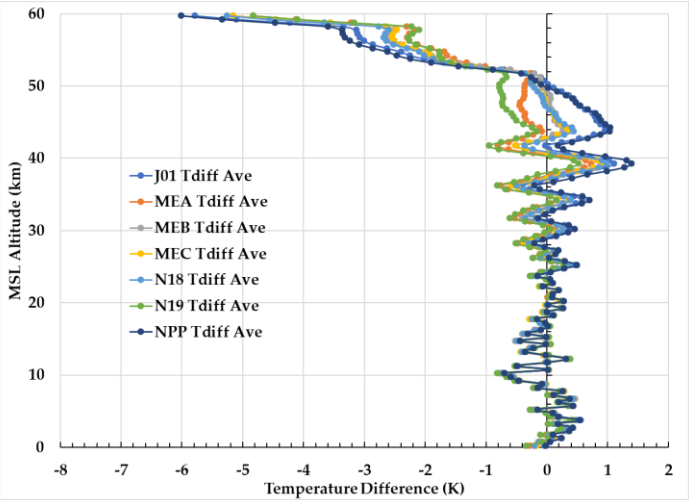

Jul 1, 2020

Water vapor difference profile at matchups between ECMWF, GNSS-RO and MW sounder data.

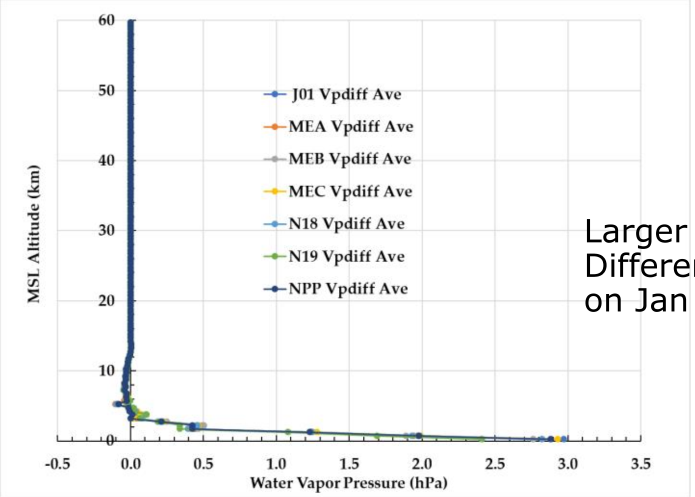

Larger Difference on Jan 1.

Jan 1, 2020

ATMS Ch 15/ AMSU-A Ch 14

ATMS Ch 10/ AMSU-A Ch 9

ATMS/AMSU-A Ch 2

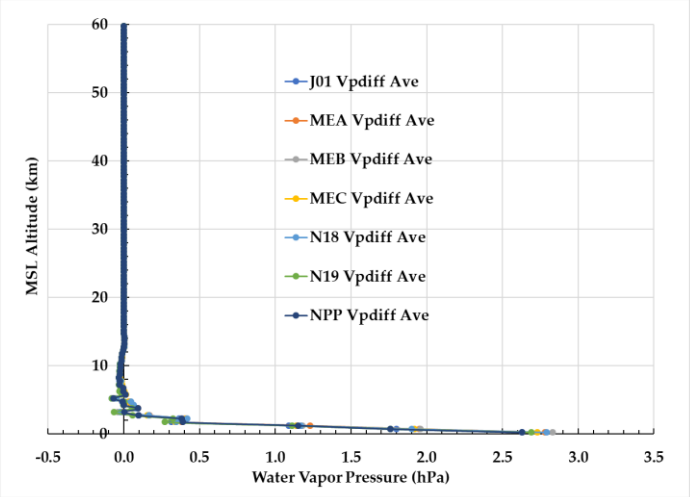

Jul 1, 2020

CRTM-simulated MW Sounder Tb Time Series (1 of 4)

CRTM-simulated Tb Parameter Definitions

- ❖ Single-sensor
  - Daily- and global-mean for S-NPP (NPP) and NOAA-20 (N20) ATMS and NOAA-18 (N18), NOAA-19 (N19), Metop A (MEA), Metop B (MEB), and Metop C (MEC) AMSU-A instruments
    - Tb using ECMWF sounding: Tb_{ECMWF}
    - Tb_{ECMWF} - Tb_{RO}: $\left(\overline{\delta Tb^{SS}}\right)_{gl}$
- ❖ Inter-sensor
  - Daily- and Global-mean between each of the 10 ATMS-to-AMSU-A instrument pairs
    - Tb_{ECMWF} - Tb_{RO} double difference: $\left(\overline{\delta Tb^{IS}}\right)_{gl}$

CRTM-simulated MW Sounder Tb Time Series (2 of 4)

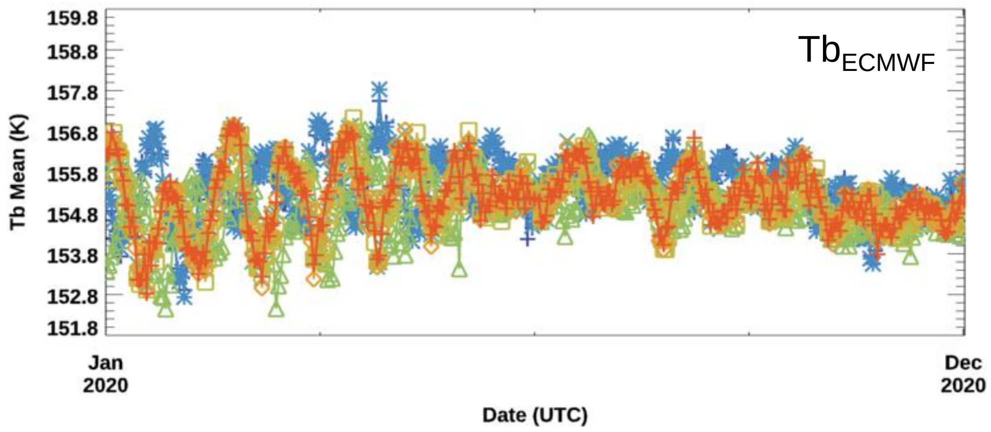

Timeseries mean ~155 K and min-to-max range ~4K

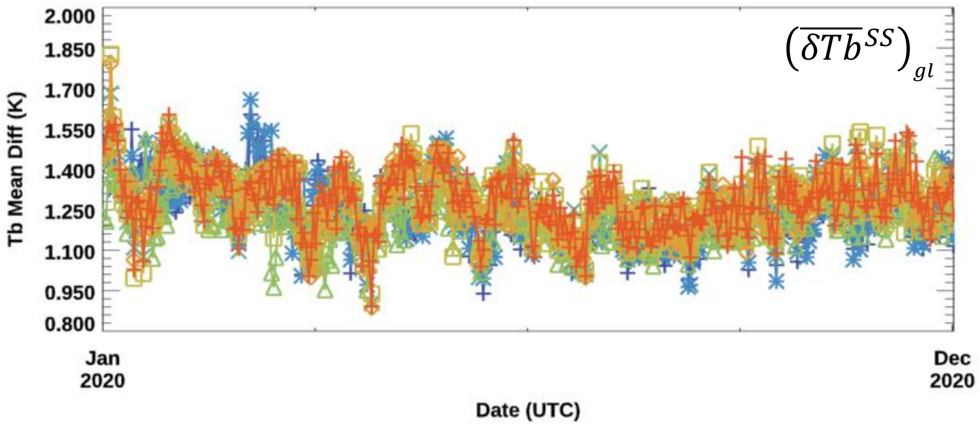

Timeseries mean ~1.25 K and min-to-max range ~0.9K

+ NPP ✳ N20 × N18 △ N19 □ MEA ◇ MEB + MEC

ATMS Ch 2/AMSU-A Ch 02

- Tb_{ECMWF} and Tb_{RO} are within about 1% of each other
- $\left(\overline{\delta Tb}^{SS}\right)_{gl}$ removes over 75% of the variability in Tb_{ECMWF} .
- $\left(\overline{\delta Tb}^{IS}\right)_{gl}$ removes almost all of the bias in $\left(\overline{\delta Tb}^{SS}\right)_{gl}$, and their difference removes about 25% of the time series variability.

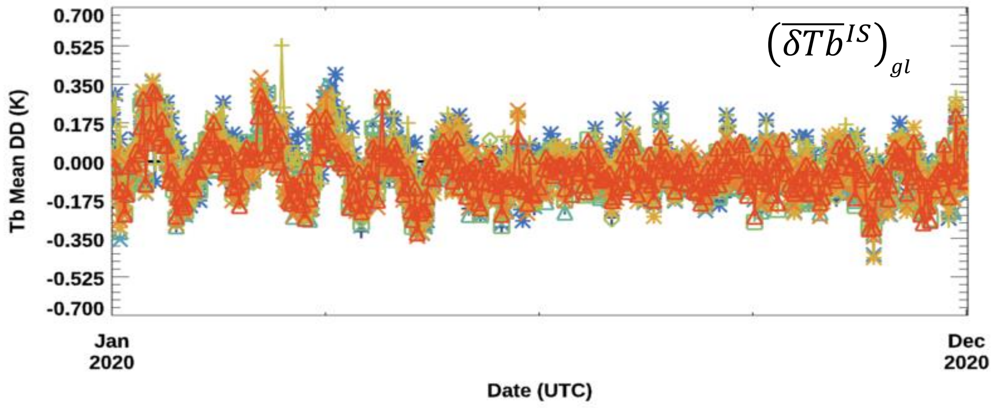

Timeseries mean ~0 K and min-to-max range ~0.7K

+ NPP-N18 ✳ NPP-N19 × NPP-MEA △ NPP-MEB □ NPP-MEC

◇ J01-N18 + J01-N19 ✳ J01-MEA × J01-MEB △ J01-MEC

CRTM-simulated MW Sounder Tb Time Series (3 of 4)

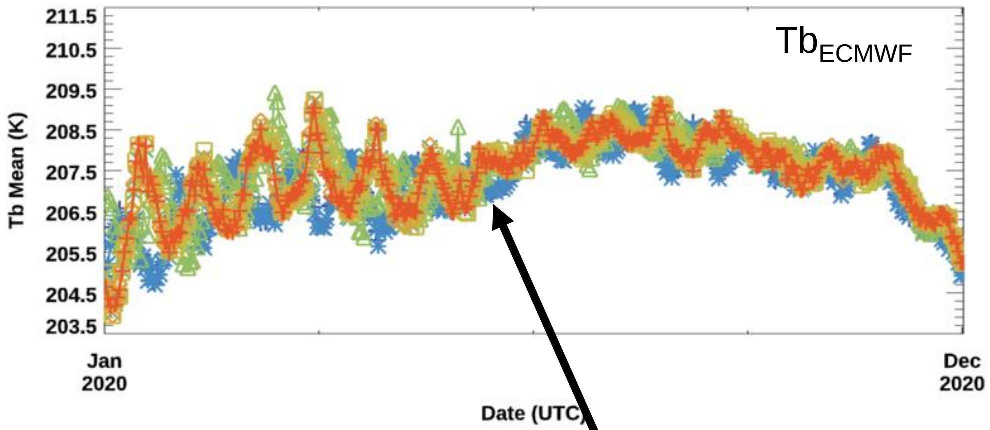

Timeseries mean ~207 K and min-to-max range ~5K

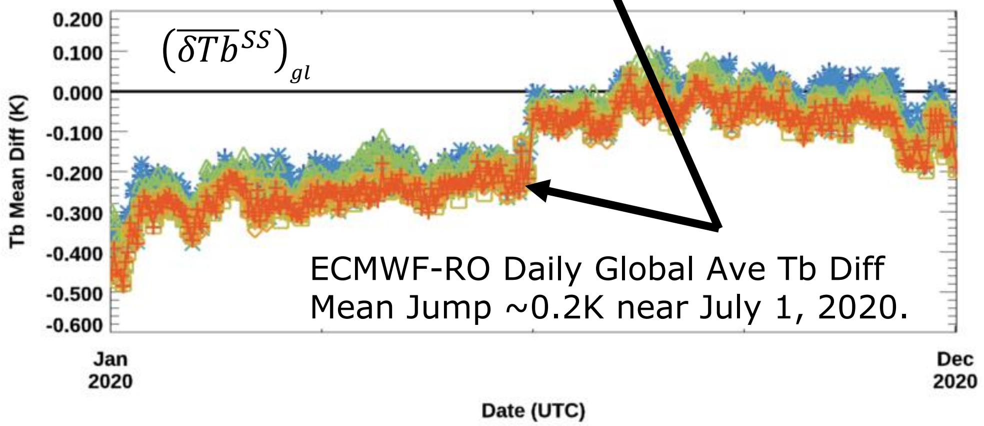

Timeseries mean ~-0.1 K and min-to-max range ~0.6K

ATMS Ch 10/AMSU-A Ch 09

- Tb_{ECMWF} and Tb_{RO} are within about 0.05% of each other
- $\left(\overline{\delta Tb^{SS}}\right)_{gl}$ removes over 90% of the variability in Tb_{ECMWF} .
- $\left(\overline{\delta Tb^{IS}}\right)_{gl}$ removes 50% of the bias in $\left(\overline{\delta Tb^{SS}}\right)_{gl}$, and their difference removes about 66% of the time series variability.
- There is a clear jump in $\left(\overline{\delta Tb^{SS}}\right)_{gl}$, which cannot be attributed uniquely to Tb_{ECMWF} or Tb_{RO}.

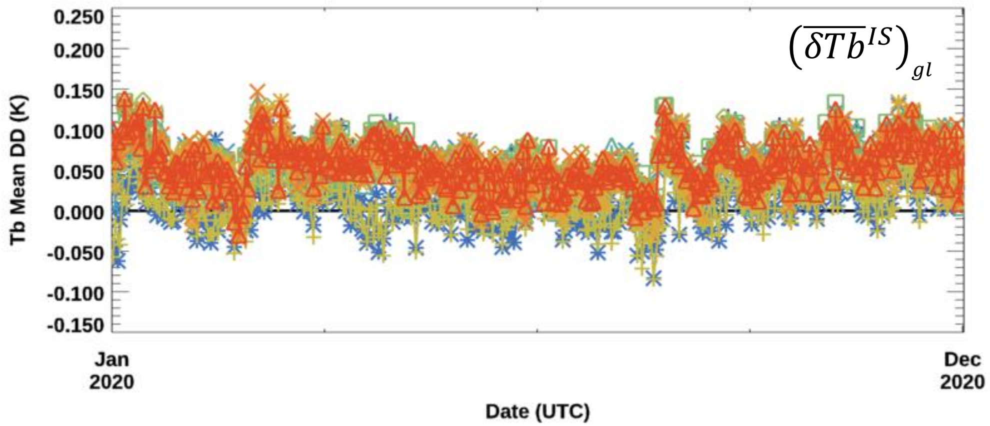

Timeseries mean ~0.05 K and min-to-max range ~0.2K

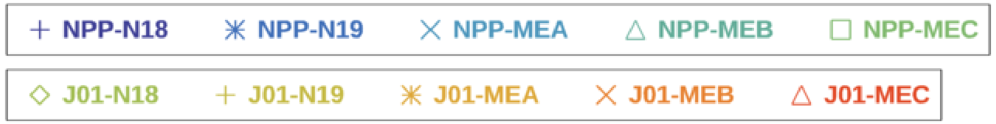

CRTM-simulated MW Sounder Tb Time Series (4 of 4)

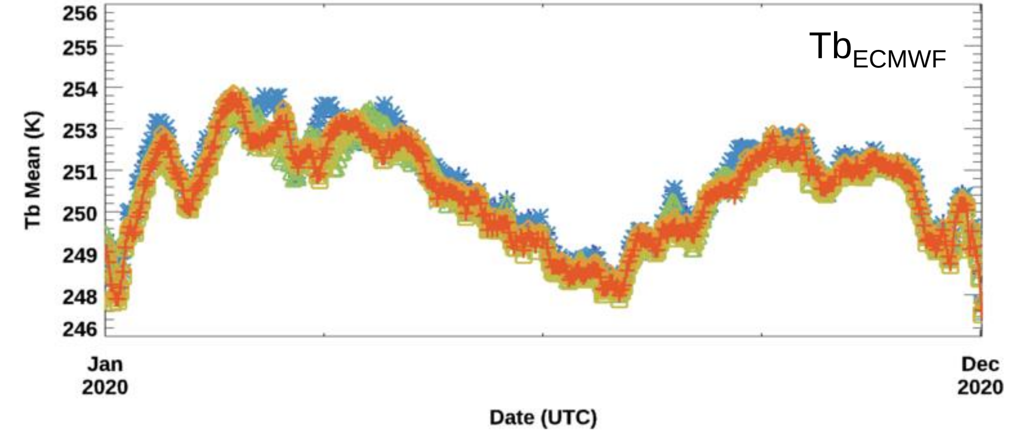

Timeseries mean ~250 K and min-to-max range ~7K

ATMS Ch 15/AMSU-A Ch 14

- Tb_{ECMWF} and Tb_{RO} are within about 0.2% of each other
- $\left(\overline{\delta Tb^{SS}}\right)_{gl}$ removes only about 29% of the variability in Tb_{ECMWF} .
- $\left(\overline{\delta Tb^{IS}}\right)_{gl}$ removes 75% of the bias in $\left(\overline{\delta Tb^{SS}}\right)_{gl}$, and their difference removes about 70% of the time series variability.

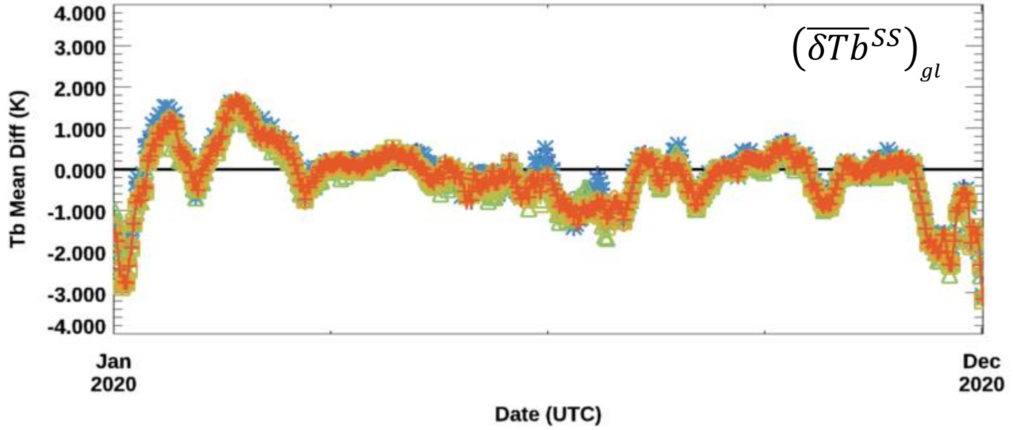

Timeseries mean ~0.5 K and min-to-max range ~5.0K

+ NPP ✳ N20 × N18 △ N19 □ MEA ◇ MEB + MEC

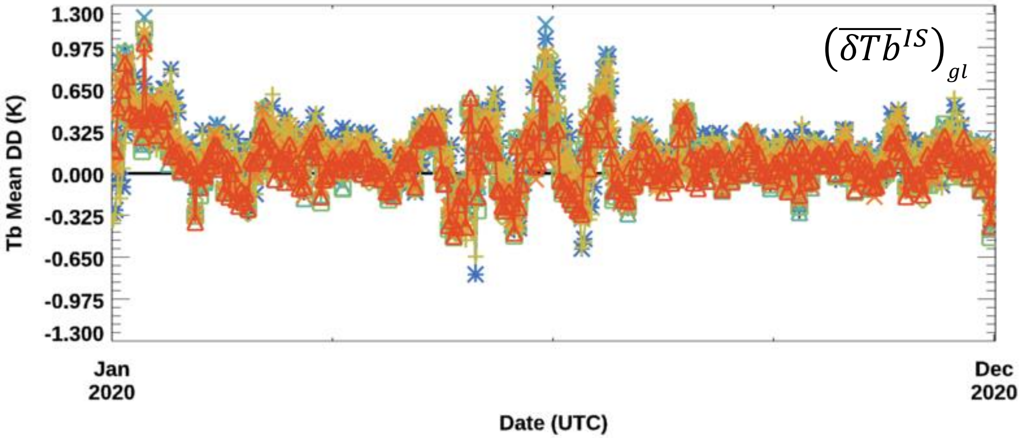

Timeseries mean ~0.125 K and min-to-max range ~1.5K

+ NPP-N18 ✳ NPP-N19 × NPP-MEA △ NPP-MEB □ NPP-MEC

◇ J01-N18 + J01-N19 ✳ J01-MEA × J01-MEB △ J01-MEC

Mean, RMS Std Dev and NSF^ Derived from Seven Single-sensor $\left(\overline{\delta Tb^{SS}}\right)_{gl}$, and 10 ATMS-to-AMSU-A Inter-sensor Pair $\left(\overline{\delta Tb^{IS}}\right)_{gl}$, Time Series Mean and Std. Dev. Values

ATMS (AMSU-A) Channel	Single-Sensor All-satellite Population			ATMS-to-AMSU-A Inter-Sensor All-satellite Population		
	Mean (K)	RMS STD (K)	NSF^	Mean (K)	RMS STD (K)	NSF^
2(2)	1.26	0.11	1E-03	-0.04	0.11	1E-04
3(3)	1.07	0.09	1E-03	0.00	0.10	1E-04
5(4)	0.24	0.05	1E-03	0.04	0.04	1E-04
6(5)	0.00	0.04	1E-04	0.03	0.03	1E-04
7(6)	-0.11	0.05	1E-04	0.02	0.02	1E-04
8(7)	-0.16	0.06	1E-03	0.02	0.02	1E-04
9(8)	-0.18	0.08	1E-03	0.02	0.02	1E-04
10(9)	-0.14	0.11	1E-03	0.05	0.03	1E-04
11(10)	-0.13	0.14	1E-03	0.06	0.04	1E-04
12(11)	-0.12	0.18	1E-03	0.07	0.07	1E-04
13(12)	-0.08	0.29	1E-03	0.08	0.11	1E-04
14(13)	0.02	0.50	1E-03	0.11	0.17	1E-03
15(14)	-0.17	0.76	1E-03	0.12	0.22	1E-03
All Channels	0.28*	0.28	1E-03	0.05*	0.10	1E-04

- Single-sensor (inter-sensor) NSF values of ~10^{-4} are found for 2 of 13 (11 of 13) channels.
- For these channels, Tb uncertainty interfere less with analysis of single- or double-difference calibration equation terms with NSF=10^{-3}.

$$^{\wedge}NSF = 10^{[INT(LOG_{10}(X)+(\alpha-1))]}$$

$$X = \frac{RMSE}{300\ K} \quad RMSE = \sqrt{Mean^2 + (RMS\ STD)^2} \quad \alpha = NINT\left[\frac{X}{INT(LOG_{10}(X))}\right]$$

NSF≈10^{-3}

NSF≈10^{-4}

*Computed as the mean of the absolute values to obtain a more realistic values of the absolute differences.

Summary

- CRTM-simulated satellite MW sensor Tb uncertainties are estimated to better understand our ability to track NOAA MW sounder data quality, and analyze their calibration anomaly mechanisms.
- Uncertainties are estimated with CRTM-simulated Tb generated separately with ECMWF ENS and GNSS RO soundings collocated with NPP and N20 ATMS, and MEA, MEB, MEC, N18 and N19 AMSU-A, operational MW sounder data locations
- Global-average ECMWF ENS and GNSS RO temperature and water vapor soundings can differ as a function of mean sea level altitude and season, which translate directly to single-sensor Tb difference variability between these simulations that have an all-channel NSF value of 10^{-3} (~0.3 K).
- ATMS-to-AMSU-A inter-sensor simulated Tb differences, derived from the double difference of single-sensor simulated Tb differences, reduce all-channel NSF to a value of 10^{-4} (~0.03 K).
- It is found that CRTM-simulation Tb uncertainty can be on the same scale as MW instrument calibration anomaly mechanisms for single sensor O-B Ta bias data, but much smaller for many inter-sensor Ta biases.

Thank You!

Any Questions??

BACKUP SLIDES

Contemporary NOAA MW Sounders

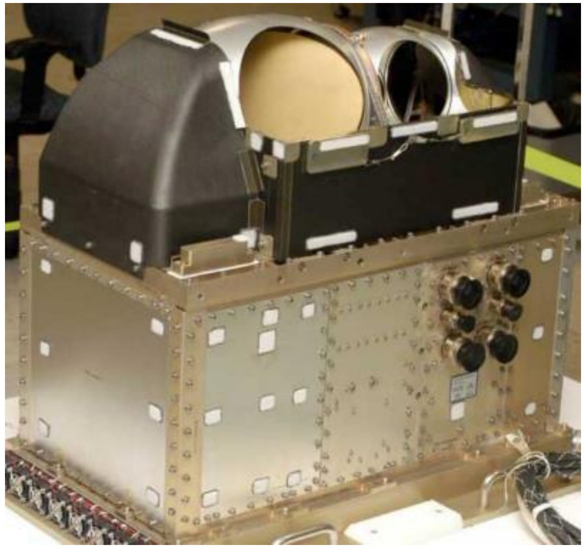

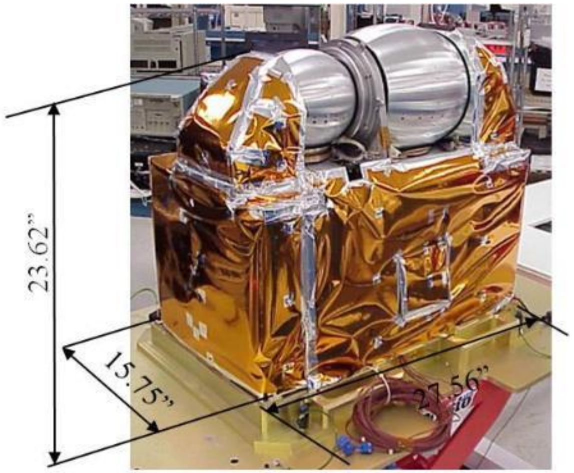

ATMS Instrument
(Images courtesy of Northrop Grumman Electronics Systems)

- The Advanced Technology Microwave Sounder (ATMS) and Advanced Microwave Sounding Unit (AMSU)/Microwave Humidity Sounder (MHS)
  - Flown on-board NASA, NOAA, and EUMETSAT polar-orbiting satellites.
  - Over 20 frequency bands centered between 23 GHz and 183 GHz
    - ✓ 23 GHz – 40 GHz (2 bands): "Window" region that senses earth-surface properties through clouds
    - ✓ 50 GHz – 60 GHz (12-13 bands): Layer-average atmospheric temperature (T) sensing region
    - ✓ 80 GHz – 183 GHz (6-7 bands): Water vapor (WV), precipitation and soil moisture sensing region

2-Point Linear Instrument Calibration with Adjustment for Weak Response Non-Linearity

Warm load (or blackbody) with NIST-Traceable Platinum Resistance Thermometers (~275 K – 285 K)

Cold Space (2.73 K)

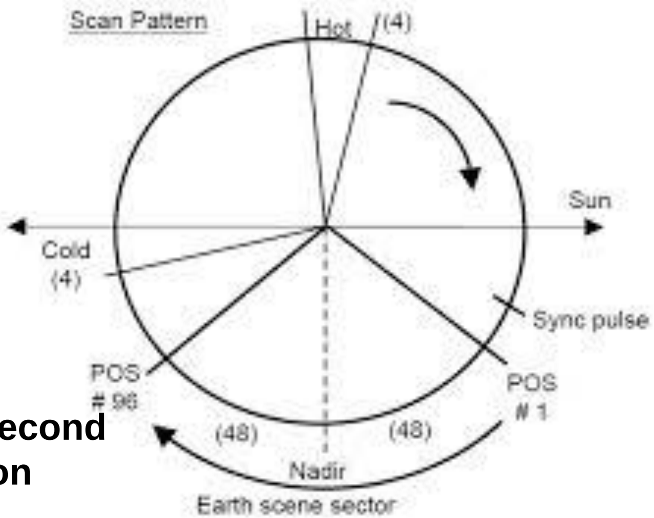

2.67 second rotation

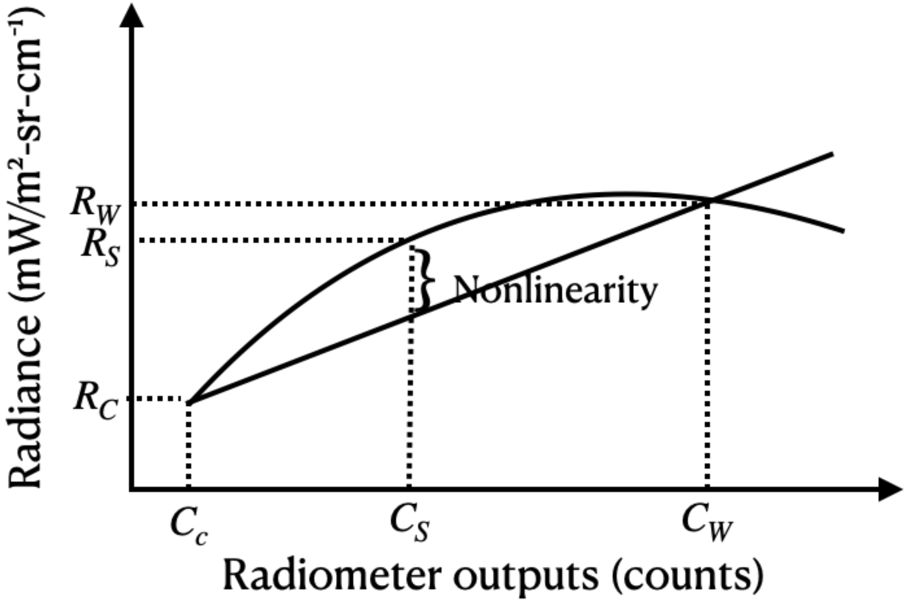

$$R = R_c + \left(\frac{R_w - R_c}{\overline{C_w} - \overline{C_c}}\right)(\overline{C_s} - \overline{C_c}) + Q$$

$$= R_c + Gain(\overline{C_s} - \overline{C_c}) + Q$$

$$Q = \frac{1}{4} T_{nlin}^{max}\left[4(x - 0.5)^2 - 1\right]$$

Cross-track Scanning Image Buildup

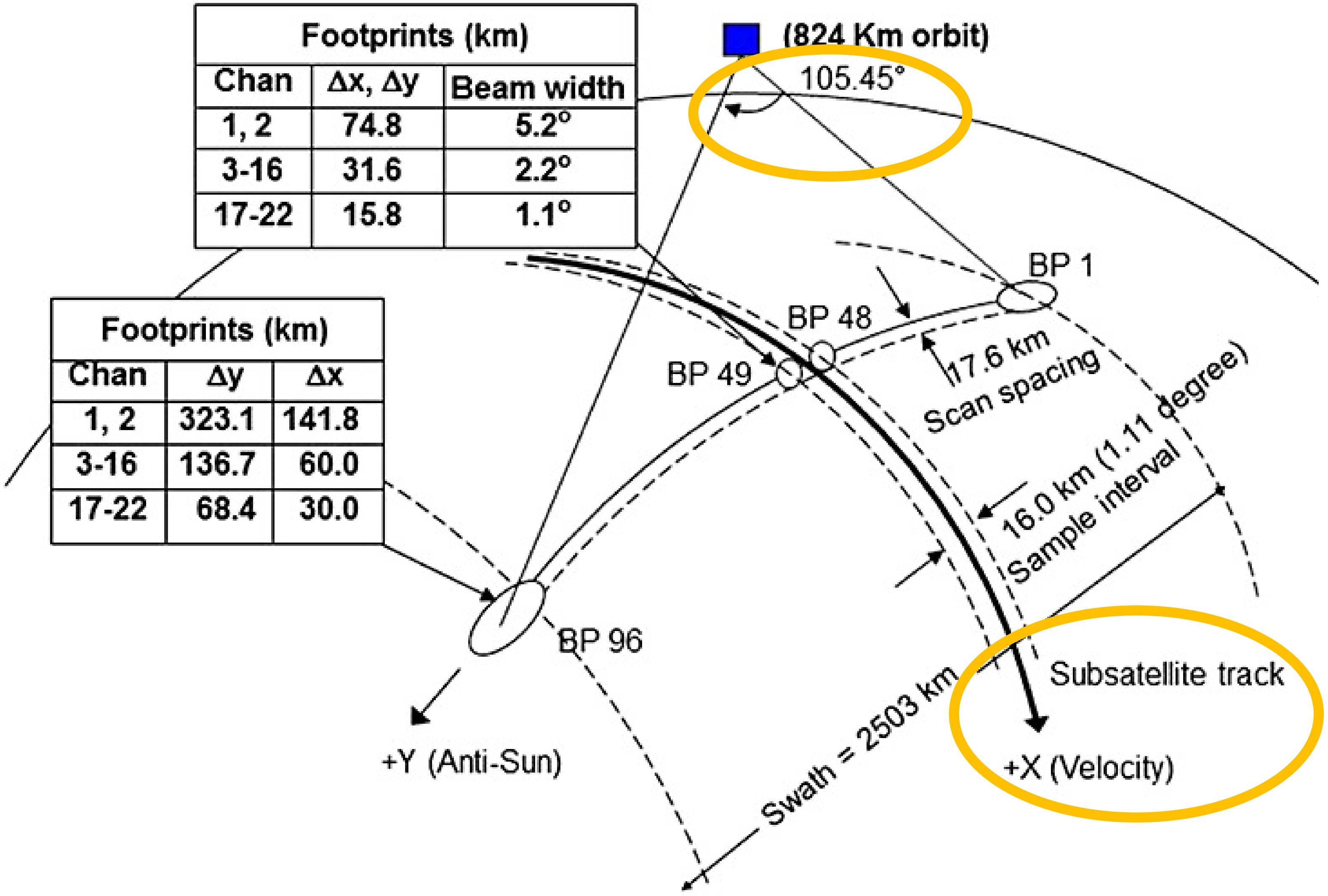

Footprints (km)		
Chan	Δx, Δy	Beam width
1, 2	74.8	5.2°
3-16	31.6	2.2°
17-22	15.8	1.1°

Footprints (km)		
Chan	Δy	Δx
1, 2	323.1	141.8
3-16	136.7	60.0
17-22	68.4	30.0

- ❖ Images created by the scanning motion of the rotating antenna and the orbital velocity of the satellite
- ❖ Larger footprints near the scan edge than at “nadir”
- ❖ Swath width is about 2500 km

22

NOAA-20 Images October 12, 2021

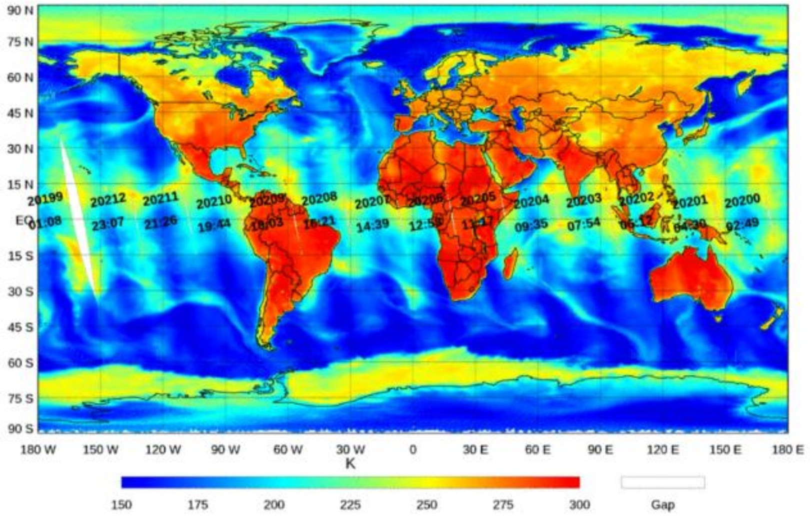

ATMS Surface “Window” 23.8 GHz

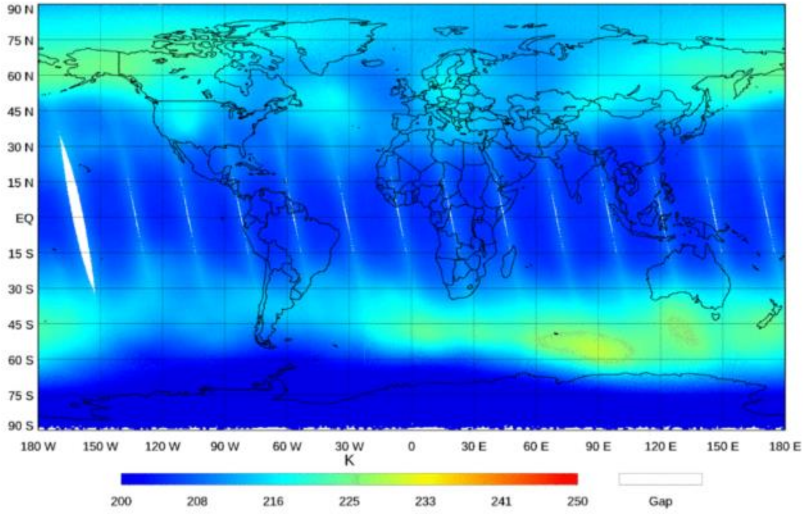

ATMS Layer T 57.29 GHz

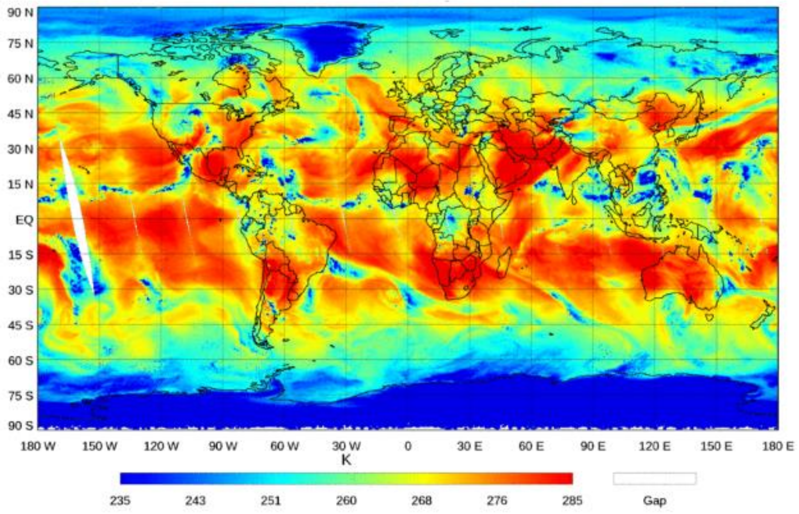

ATMS Layer WV and Precipitation 183.31±7 GHz

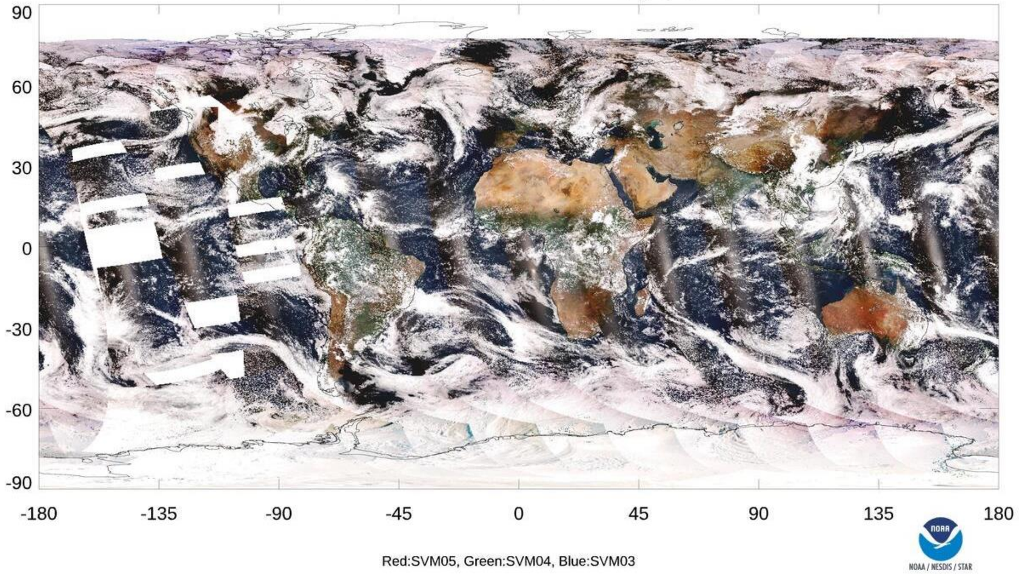

True color image from the Visible Infrared Visible Infrared Imaging Radiometer Suite (VIIRS) reveals the complimentary information from MW instruments.

23